JCI insight

RESEARCH ARTICLE

IFN-γ is a therapeutic target in paraneoplastic cerebellar degeneration

Lidia Yshii,[1] Béatrice Pignolet,[1,2] Emilie Mauré,[1] Mandy Pierau,[3] Monika Brunner-Weinzierl,[3] Oliver Hartley,[4] Jan Bauer,[5] and Roland Liblau[1]

[1]Centre de Physiopathologie Toulouse-Purpan (CPTP), Université de Toulouse, CNRS, Inserm, UPS, Toulouse, France. [2]Department of Clinical Neurosciences, Toulouse University Hospital, Toulouse, France. [3]Department of Experimental Pediatrics, University Hospital, Otto-von-Guericke University, Magdeburg, Germany. [4]Department of Pathology and Immunology, Faculty of Medicine, University of Geneva, Geneva, Switzerland. [5]Department of Neuroimmunology, Center for Brain Research, Medical University of Vienna, Vienna, Austria.

Paraneoplastic neurological disorders result from an autoimmune response against neural self-antigens that are ectopically expressed in neoplastic cells. In paraneoplastic disorders associated to autoantibodies against intracellular proteins, such as paraneoplastic cerebellar degeneration (PCD), current data point to a major role of cell-mediated immunity. In an animal model, in which a *neo*–self-antigen was expressed in both Purkinje neurons and implanted breast tumor cells, immune checkpoint blockade led to complete tumor control at the expense of cerebellum infiltration by T cells and Purkinje neuron loss, thereby mimicking PCD. Here, we identify 2 potential therapeutic targets expressed by cerebellum-infiltrating T cells in this model, namely α4 integrin and IFN-γ. Mice with PCD were treated with anti-α4 integrin antibodies or neutralizing anti–IFN-γ antibodies at the onset of neurological signs. Although blocking α4 integrin had little or no impact on disease development, treatment using the anti–IFN-γ antibody led to almost complete protection from PCD. These findings strongly suggest that the production of IFN-γ by cerebellum-invading T cells plays a major role in Purkinje neuron death. Our successful preclinical use of neutralizing anti–IFN-γ antibody for the treatment of PCD offers a potentially new therapeutic opportunity for cancer patients at the onset of paraneoplastic neurological disorders.

Introduction

Paraneoplastic neurological disorders are rare immune-mediated diseases that develop in the setting of malignancy and offer a unique prospect to analyze the interplay between tumor immunity and autoimmunity (1). In those diseases, the pathogenic adaptive immune response targets proteins, so-called onconeural antigens, which are expressed physiologically by neural cells and aberrantly by tumor cells (2). Highly specific anti-neuronal autoantibodies in the serum and cerebrospinal fluid (CSF) represent key diagnostic biomarkers of these diseases. Paraneoplastic cerebellar degeneration (PCD) is characterized by the selective loss of Purkinje neurons in the cerebellum (3). The hallmark of PCD is the production of high titers of antibodies against intracellular proteins of Purkinje cells, most frequently cerebellar degeneration-related antigen (CDR2/CDR2L), also known as Yo antibodies (4). It has also been reported that effector cytotoxic CD8 T cells able to produce IFN-γ in response to CDR2 circulate in the blood and CSF of patients (3). PCD develops mostly in female patients with gynecologic (ovarian or breast) carcinomas that express the Purkinje neuron–specific CDR2/CDR2L protein (3–5). Although the occurrence of PCD is rare (about 10 new cases/year in France) (6), the risk for such complication may increase with application of immunotherapy for these malignancies (7, 8), thereby pointing to paraneoplastic neurological disorders as potential side effects of immune checkpoint blockade. Consistent with this hypothesis, the development of PCD after CTLA-4 blockade was observed in a mouse model expressing a model onconeural antigen both in Purkinje neurons and in implanted breast cancer cells (9). The enhanced tumor control by immune checkpoint therapy was obtained at the expense of autoimmune PCD, with accumulation of T cells within the cerebellum and subsequent neurodegeneration (9).

To identify therapeutic approaches for PCD, for which there is currently no specific and effective treatment, we used a preclinical validation approach using our recently developed animal model of PCD.

Conflict of interest: The authors have declared that no conflict of interest exists.

Submitted: December 21, 2018
Accepted: February 21, 2019
Published: April 4, 2019.

Reference information: JCI Insight. 2019;4(7):e127001. https://doi.org/10.1172/jci.insight.127001.

We observed abundant IFN-γ secretion by cerebellum-infiltrating T cells upon recognition of the model onconeural antigen. This initiated a feed-forward loop through upregulation of MHC class I molecules on Purkinje cells, rendering them vulnerable to direct killing by antigen-specific CD8 T cells. Antibody-mediated neutralization of IFN-γ in the mouse PCD model resulted in protection of Purkinje neurons from immune-mediated killing, identifying a potential therapeutic option for patients at the early stages of PCD.

Results

Identification of therapeutic targets in a preclinical model of PCD. We used a mouse model of PCD, thereafter called L7-HA-PCD, in which a *neo*–self-antigen (hemagglutinin; HA) is expressed both in Purkinje neurons and in implanted breast tumor cells. In this model, anti–CTLA-4 mAb therapy enhances tumor control at the expense of autoimmune PCD (9). Moreover, cerebellum-infiltrating CD8 T cells elicit neuronal cell death, and accordingly, they are in close contact with soma and dendrites of Purkinje neurons (Figure 1A) (9). Since this model could mimic key aspects of the human disease, we reasoned that it could also be useful to identify and validate therapeutic targets in vivo. By comparing expression of effector molecules by cerebellum-infiltrating T cells vs. their peripheral counterparts, we searched for molecules expressed by the disease-relevant T cells. We focused on molecules involved in CD8 T cell migration to the CNS and in CD8 T cell effector functions that could be therapeutically targeted. The α4 integrin (CD49d) was strongly expressed on approximately 40% of CD4 and CD8 T cells invading the cerebellum of L7-HA-PCD mice, whereas T cells in the secondary lymphoid organs expressed lower levels of this integrin (Figure 1B). Additionally, cerebellum-infiltrating T cells from L7-HA-PCD mice released abundant IFN-γ upon recognition of HA, the model onconeural antigen (Figure 1C). In contrast, few CD4 T and almost no CD8 T cells from the spleen or cervical lymph nodes (cLN) of L7-HA-PCD mice reacted ex vivo to HA peptides (Figure 1C). To investigate whether an IFN-γ–mediated signaling cascade was activated in Purkinje neurons, we assessed both phosphorylation and nuclear translocation of the transcription factor STAT1, a key signaling molecule downstream the IFN-γ receptor. Purkinje neuron nuclei (10 of 10 neurons) in L7-HA-PCD mice, but none (out of 10) in control animals, showed strong nuclear staining for phosphorylated STAT1 (pSTAT1) (Figure 1D). These observations suggest a T cell–driven IFN-γ receptor/pSTAT1 signaling pathway in Purkinje neurons. Upregulation of MHC class I molecules on Purkinje cells was previously noted in the L7-HA-PCD model and was associated with CD8 T cell–mediated killing (9). To evaluate the link between IFN-γ signaling and MHC class I expression in Purkinje neurons, we used cerebellar slice cultures. Upon treatment with IFN-γ, a clear expression of MHC class I molecules became detectable at the cell surface of all 33 Purkinje neurons, whereas none (out of 20) express detectable levels of MHC class I in the absence of IFN-γ (Figure 1E). Finally, in the cerebellum of 2 postmortem samples of patients with PCD, although the Purkinje cells were totally eliminated, few focal areas with inflammation and pSTAT1$^+$ neurons and glial cells were identified (Figure 1F). In the cerebellar peduncle of the anti-Yo case, 0.9 neurons/mm^2 and 12 glial cells/mm^2 stained for pSTAT1. In the molecular and granular layer of the anti-Ma2 case, 2.0 neurons/mm^2 and 9.5 glial cells/mm^2 stained for pSTAT1. No staining for pSTAT1 was found in control cerebellum.

Altogether, our findings identified α4 integrin and IFN-γ as potential therapeutic targets in our mouse model, and we, thus, designed in vivo experiments to validate or invalidate them.

Treatment with anti-α4 integrin mAb or CCR5 antagonist shows no efficacy in the PCD model. Since anti-α4 integrin therapy is efficient and approved for another immune-mediated central neurological disease, namely multiple sclerosis (10), we evaluated whether treatment with anti-α4 integrin mAb could protect Purkinje neurons from immune-mediated death in the L7-HA-PCD model. L7-HA-PCD recipients were treated with an anti-α4 integrin mAb (PS/2) or a control IgG starting on day 10 after the disease induction (Supplemental Figure 1A; supplemental material available online with this article; https://doi.org/10.1172/jci.insight.127001DS1). In both groups, the tumor remained well controlled (Figure 2A). However, mice treated with the anti-α4 integrin mAb exhibited a similar weight loss (Figure 2B) and reduced motor coordination (Figure 2C) compared with the IgG-treated control animals, suggesting unabated PCD. Indeed, loss of Purkinje neurons was as profound in anti-α4 integrin–treated mice as in control mice (Figure 2D). As a reference, the mean (± SD) number of Purkinje cells was 29.88 ± 2.48/mm in 28 WT mice (9), very similar to values reported by others (11, 12). T cell infiltration in the cerebellum was modestly and not significantly ($P = 0.27$) decreased in mice treated with the anti-α4 integrin mAb (324.4 ± 125.5/mm^2; $n = 8$ mice) vs. mice treated with the control antibody (511.3 ± 134.8/mm^2;

n = 8 mice). Using an established and efficient treatment regimen (13), these data indicate that the anti-α4 integrin therapeutic approach is not efficient at blocking ongoing disease, at least in our model of PCD. The CCR5 chemokine receptor has been implicated in immune cell recruitment in several inflammatory diseases of the CNS (14). Although it was not highly expressed on cerebellum-infiltrating T cells at day 16 (Supplemental Figure 2A), we investigated whether CCR5 signaling was required for disease development. Treatment of L7-HA-PCD mice with a CCR5 antagonist (5P12-RANTES) starting on day 10 after disease induction did not block development of PCD and Purkinje neuron destruction, as shown in Supplemental Figure 2, B–E. This antagonist was, however, efficient to restrict brain inflammation but not spinal cord inflammation in a model of experimental autoimmune encephalomyelitis (EAE) following juvenile virus infection in mice (D. Merkler [Department of Pathology and Immunology, University of Geneva, Switzerland], personal communication).

Neutralization of IFN-γ at PCD onset prevents clinical manifestations and elimination of Purkinje neurons. Since interfering with T cell migration did not mitigate pathology, we thought of an alternative strategy that would aim at interfering with the effector mechanisms of CNS-infiltrating T cells. As IFN-γ release and signaling occurred within the cerebellum, we decided to test the effect of IFN-γ inhibition. L7-HA-PCD mice were treated with a neutralizing anti–IFN-γ antibody (XMG1.2) or an isotype control from day 10 after disease induction onward, hence avoiding interference with the induction and expansion of the HA-specific T cell response and the immune-mediated tumor control (Figure 3A). Strikingly, IFN-γ neutralization protected mice from the clinical manifestations of PCD, namely weight loss (Figure 3B), and reduced motor performance (Figure 3C). In addition, histological analysis revealed that IFN-γ blockade prevented T cell–mediated Purkinje cell death (Figure 3D). These results show that administration of the anti–IFN-γ antibody at the onset of clinical disease halted the development of PCD without impairing the antitumor response. However, IFN-γ blockade from induction of disease (day 0) in L7-HA mice prevented the development of the beneficial antitumor immune response, resulting in the absence of PCD development (Supplemental Figure 3, A–D).

Given the importance of IFN-γ in the development of the mouse model of PCD, we investigated whether the HA-specific CD8 T cells, which are in close interaction with the Purkinje neurons, could be an essential cellular source of IFN-γ. For that, we transferred IFN-γ–deficient HA-specific CD8 together with HA-specific CD4 T cells. The lack of IFN-γ on these specific cells did not abrogate PCD progression (Figure 3E).

T cell infiltration is reduced in the cerebellum of L7-HA-PCD mice treated with anti–IFN-γ mAb. To understand the mechanisms whereby neutralization of IFN-γ inhibited PCD development, we analyzed quantitatively and qualitatively the cerebellum-infiltrating T cells. On day 20, reduced $CD3^+$ T cell infiltration was observed in the cerebellum of mice treated with anti–IFN-γ mAb from day 10 onward compared with mice treated with the isotype control (Figure 4A). We next compared the number, phenotype, and functional property of cerebellum-infiltrating T cells from L7-HA-PCD mice treated or not treated with anti–IFN-γ mAb by flow cytometry (Supplemental Figure 1B). Sixteen days after PCD induction, a marked reduction in the numbers of cerebellum-infiltrating CD4 and CD8 T cells was observed in L7-HA-PCD mice treated with anti–IFN-γ mAb (Figure 4B). The $CD4^-CD8^-Thy1.2^+$ CNS-infiltrating cells could be innate lymphoid cells, γδT cells, or αβ CD8 T cells that have downregulated the CD8 molecule (15). Upon IFN-γ neutralization, cerebellum-infiltrating CD8 T cells expressed high levels of the α4 integrin chain, potentially contributing to their residual recruitment within the CNS (Figure 4C). We then assessed the functional potential of antigen-specific T cells in L7-HA-PCD mice treated or not treated with anti–IFN-γ mAb. In both groups, a similar proportion of cerebellum-infiltrating CD4 and CD8 T cells reacted ex vivo to HA peptide by producing IFN-γ (Figure 4D). As a potential consequence of reduced density of MHC class I–HA peptide complexes on Purkinje cells, we assessed both proliferation and death of cerebellum-infiltrating T cells. Although there was no difference in the proportion of T cells expressing the proliferation marker Ki67 (Figure 4E), a nonsignificant trend for increased cell death was noted for cerebellum-infiltrating CD8 T cells (Figure 4F). No difference was observed in the frequency of $CD107a^+CD4^+$, $CD107a^+CD8^+$, and Granzyme B^+CD8^+ cells between the XMG1.2- and isotype-treated mice (Figure 4, G and H). Overall, these data suggest that the anti–IFN-γ antibody treatment resulted in partial but significant inhibition of T cell accumulation into the cerebellum of L7-HA-PCD mice.

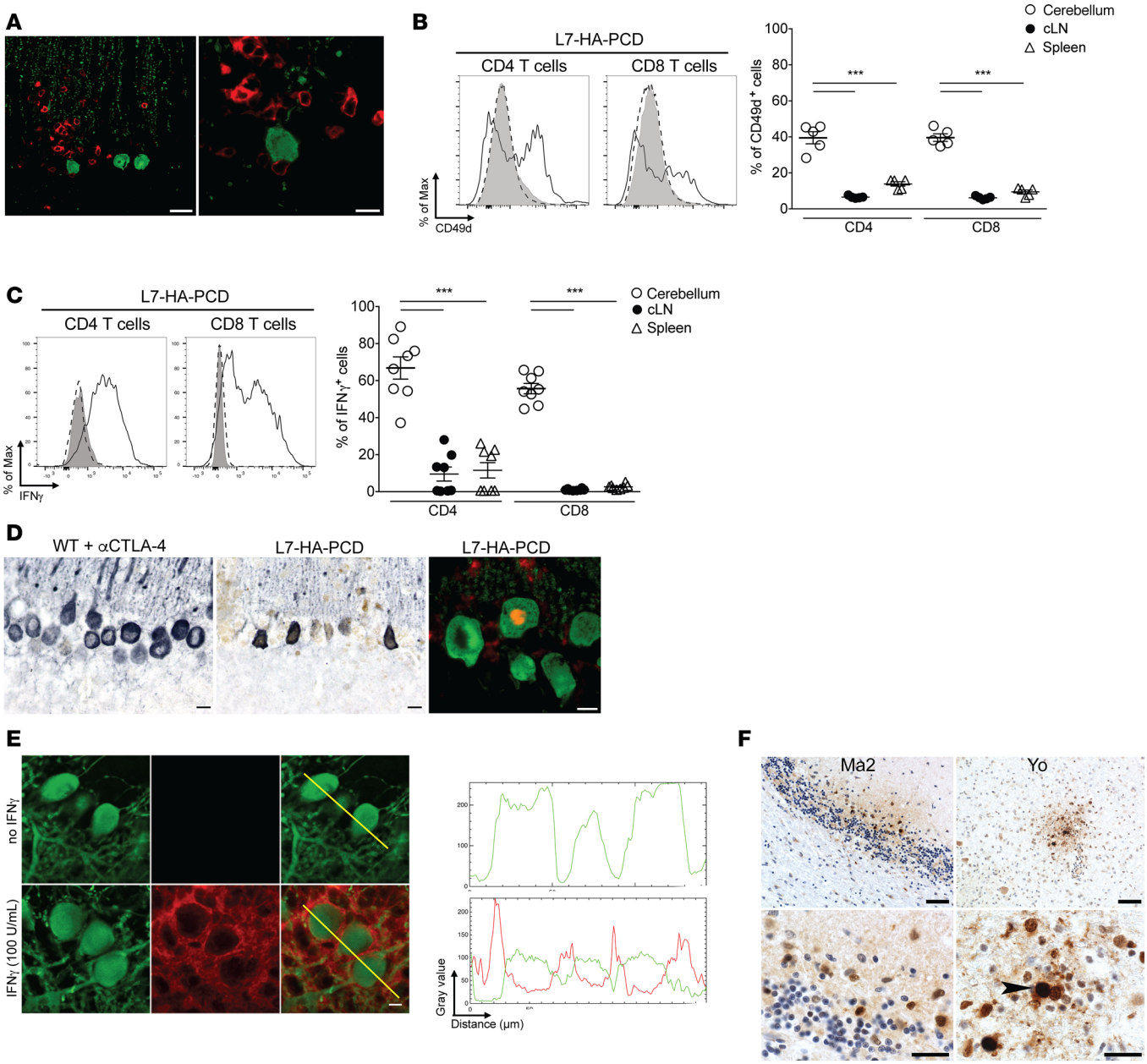

Figure 1. Identification of therapeutic targets in a mouse model of PCD. (**A**) Left: CD8 (red) and Calbindin (green) in the cerebellum of a L7-HA-PCD mouse, 20 days. Scale bar: 25 μm. Right: enlargement of left shows 2 T cells in close apposition to a calbindin$^+$ Purkinje cell. Scale bar: 10 μm. (**B**) Flow cytometry of α4 integrin (CD49d) expression on CD4 and CD8 T cells (CD90.2$^+$) from the cerebellum and secondary lymphoid organs of L7-HA-PCD mice, 16 days after 4T1-HA tumor challenge and anti–CTLA-4 mAb (αCTLA-4) therapy. Left: dotted line, spleen; gray, cervical lymph nodes (cLN); solid line, cerebellum. Right: frequency of CD49d-positive cells among CD4 and CD8 T cells from spleen, cLN, and cerebellum of 5 L7-HA-PCD mice. Paired 2-tailed *t* test, $^{***}P < 0.001$. (**C**) Flow cytometry of IFN-γ expression in CD4$^+$ and CD8$^+$ T cells from the cerebellum and secondary lymphoid organs of L7-HA-PCD mice, following in vitro stimulation with the $HA_{110–119}$ and $HA_{512–520}$ peptides for 16 hours. Left: dotted line, spleen; gray, cLN; solid line, cerebellum. Right: frequency of IFN-γ–expressing cells in CD4 and CD8 T cells (CD90.2$^+$) from 8 L7-HA-PCD mice. Paired 2-tailed *t* test, $^{***}P < 0.001$. (**D**) pSTAT1 (brown) and calbindin (blue-gray) on cerebellar sections of WT (left, WT; not expressing HA in Purkinje cells) and L7-HA-PCD mice (middle). Scale bar: 10 μm. Staining for Calbindin (green) and pSTAT1 (red) shows upregulation of pSTAT1 in the nucleus of a Purkinje cell (right). Scale bar: 7.5 μm. (**E**) Left: ex vivo cerebellar slices from L7-HA mice treated or not with IFN-γ (100 U/ml) for 24 hours and stained with an anti-calbindin antibody (green) and an anti–H2-K^d antibody (red). Scale bar: 20 μm. Right: densitometric analysis of calbindin and H2-K^d staining of Purkinje cells. Yellow lines: segments of Purkinje cells submitted to densitometric analysis of calbindin and H2-Kd staining (right panels). (**F**) Top left: pSTAT1 staining in the cerebellum of an anti-Ma2 case. Bottom left: enlargement of top left. pSTAT1 upregulation in the nuclei of microglial cells, astrocytes, and some of the granular neurons. Top right: local pSTAT1 in the cerebellar peduncle of an anti-Yo case. Bottom right: pSTAT1 is upregulated in various glial cells. In addition, pSTAT1 can be seen in the nucleus of a neuron (arrowhead). Scale bar: 50 μm (top left and right) and 20 μm (bottom left and right).

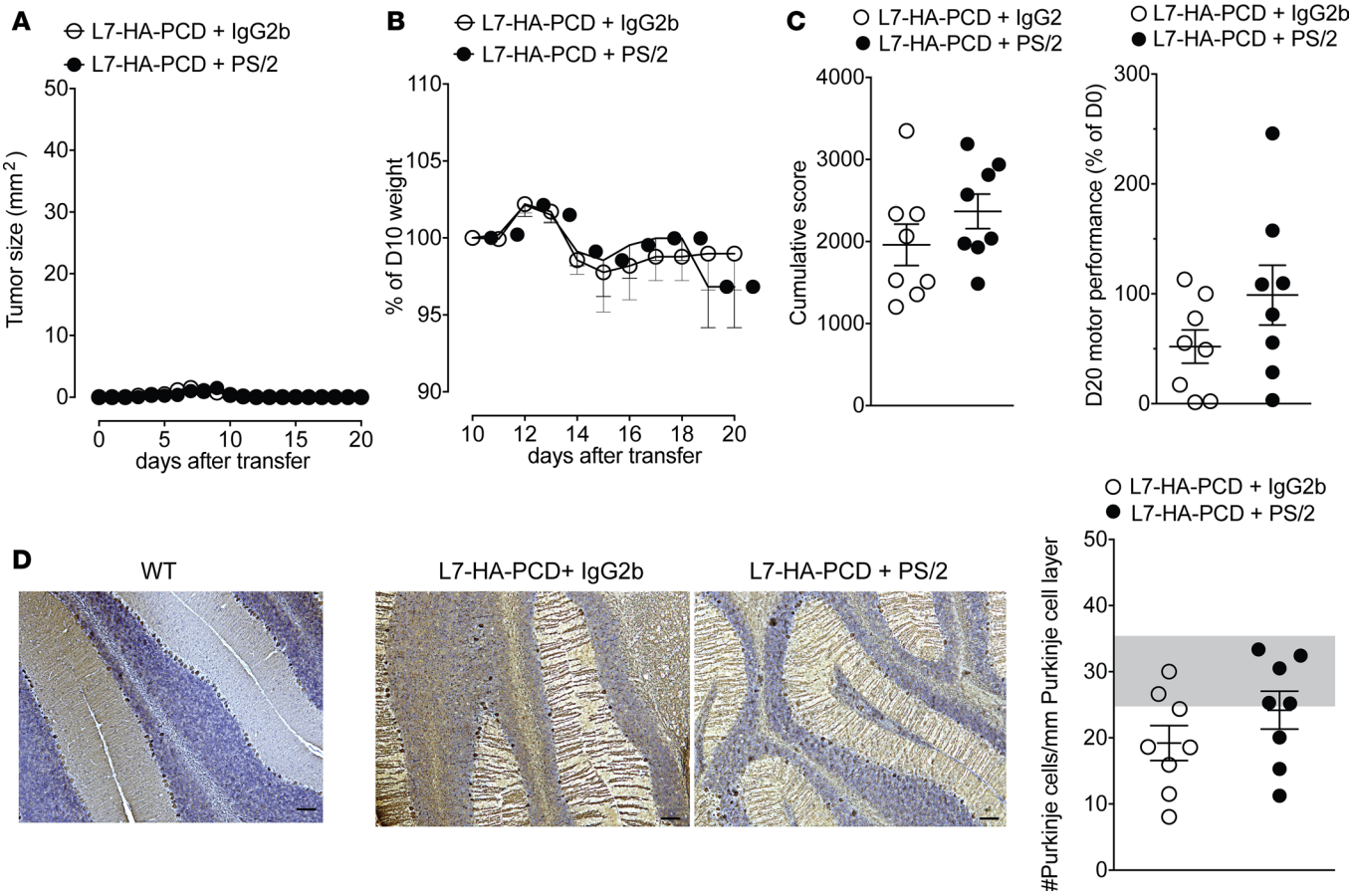

Figure 2. Treatment with an anti–α4 integrin mAb shows no efficacy in the PCD model. (**A**) Tumor size, (**B**) mouse weight loss, and (**C**) rotarod cumulative score (left) and performance on day 20 (right) of L7-HA-PCD mice treated with PS/2 (anti–α4 integrin mAb) or control IgG2b from day 10 after the induction of disease onward (*n* = 8/group, 2 independent experiments). (**D**) Left: representative staining for calbindin (violet) and nuclear counterstaining with hematoxylin (blue) on cerebellar sections from a control WT mouse, and from L7-HA-PCD mice treated with isotype control or PS/2. Scale bar: 100 μm. Right: quantitative assessment of Purkinje cell density in L7-HA-PCD mice treated with IgG2b or PS/2 (*n* = 8/group, 2 independent experiments). The shaded area represents the normal range in WT mice, meaning mean ± 2SD.

Discussion

Using a mouse model of PCD, we show that Purkinje neurons— attacked by IFN-γ–producing cytotoxic CD8 T cells — signal through the IFN-γ receptor, as shown by phosphorylation and nuclear translocation of STAT1. As a result, Purkinje neurons increase their expression of MHC class I molecules and may exhibit higher vulnerability to cytotoxic T cell attack (16). Blocking this process using an IFN-γ–neutralizing antibody prevented destruction of the neurons and limited T cell infiltration of the cerebellum. Our present study identifies IFN-γ as a targetable molecule in the mouse model of PCD and, possibly, in the human disease.

Human PCD, which is likely mediated by autoimmune response of T cells against Purkinje cell antigens CDR2/CDR2L, is characterized by development of severe cerebellar dysfunction (5). The onset is rapid, and patients are often harshly incapacitated and bedridden 3 months after the diagnosis, due to progression of ataxia, dysarthria, and, in some cases, nystagmus (17). The involvement of T cells has been suggested in this severe autoimmune neurological disease. Indeed, postmortem lesions show a clear immune cell infiltration of the cerebellum, mostly by CD8 T cells (18). Interestingly, IFN-γ–producing CD8 T cells have been detected in the blood of patients with PCD upon stimulation with CDR2 peptides (3). Additionally, CDR2/CDR2L-specific CD8 cytotoxic T cells are present in the CSF of PCD patients (3, 19), and they can kill target cells in an HLA-restricted manner (20). In addition to activated CD8 T cells, macrophages, NK cells, and CD4 Th1 T cells can also secrete large amounts of IFN-γ (21, 22).

IFN-γ likely plays a critical role in other autoimmune diseases, such as systemic lupus erythematous (SLE), multiple sclerosis, and Rasmussen encephalitis (23–25). The locally released IFN-γ profoundly alters the biology of neurons, promoting phagocyte recruitment through their production of chemokines

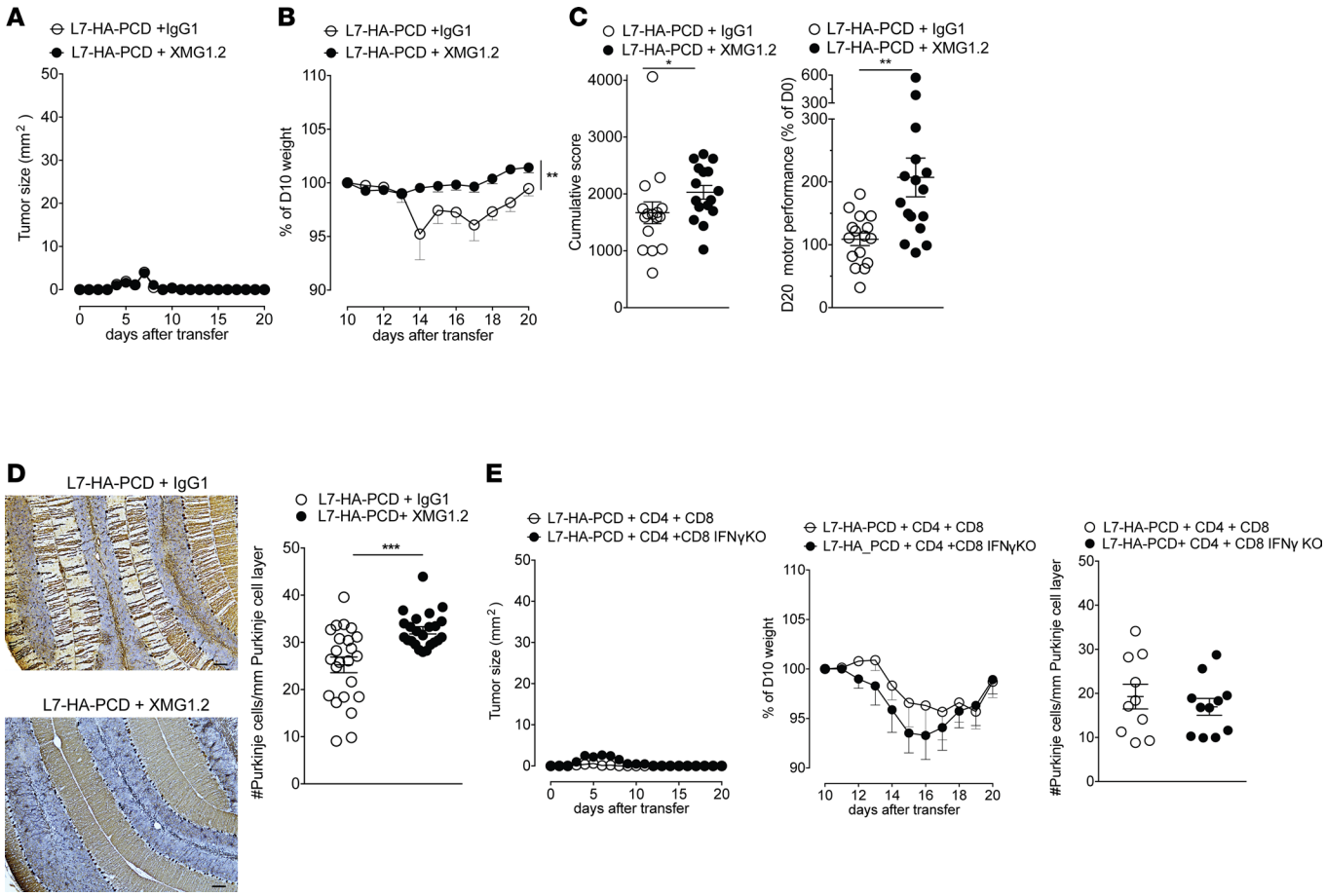

Figure 3. IFN-γ neutralization at disease onset prevents Purkinje cell loss and clinical disease. (**A**) Tumor size, and (**B**) mouse weight loss of L7-HA-PCD mice treated with XMG1.2 (neutralizing anti–IFN-γ mAb) or control IgG1 from day 10 onward (n = 23 per group, 4 independent experiments; 2-way ANOVA post-hoc Sidak's multiple comparison test, $^{**}P < 0.01$). (**C**) Rotarod performance of L7-HA-PCD mice treated with XMG1.2 or control IgG1 (n = 16 mice per group, 3 independent experiments; Mann-Whitney U test, $^{*}P < 0.05$; $^{**}P < 0.01$). (**D**) Histological analysis at day 20 of the cerebellum of L7-HA-PCD mice treated with XMG1.2 or IgG1, from day 10 onward. Left: representative staining for calbindin (brown) and nuclear counterstaining with hematoxylin (blue). Scale bar: 100 μm. Right: quantitative assessment of Purkinje cell density in L7-HA-PCD mice treated with XMG1.2 or IgG1 (n = 23 mice per group from 4 independent experiments; Mann-Whitney U test, $^{***}P < 0.01$). (**E**) IFN-γ deficiency in Purkinje cell–specific CD8 T cells does not prevent the development of the PCD mouse model. Left, tumor size; middle, weight; and right, Purkinje cell density in L7-HA-PCD mice transferred with HA-specific CD4 T cells and either IFN-γ–sufficient or IFN-γ–deficient (CD8 IFN-γ–KO) HA-specific CD8 T cells; n = 10–11 mice per group, 2 independent experiments.

and upregulation of MHC class I expression in neurons that renders them susceptible to CD8-mediated killing (16, 26, 27). Notably, upregulation, phosphorylation, and nuclear translocation of STAT1 were observed in the surviving Purkinje cells of PCD mice, indicative of IFN-γ signaling within neurons. Recently, it was shown that neuronal STAT1 signaling upon CD8 T cell attack is crucial for synaptic loss and neurological disease. Animals lacking STAT1 in neurons were therefore protected from neurodegeneration and synapse loss (27). To reinforce the importance of the IFN-γ pathway in the pathophysiology of PCD, we showed pSTAT1^{+} areas in the cerebellum of the Ma2 and Yo patients.

Immune cell infiltration into the CNS can be prevented by blocking α4β1 integrin in murine model of multiple sclerosis (MS) (28, 29). Natalizumab, a humanized α4 integrin blocking antibody, was developed for the treatment of relapsing-remitting MS, where it efficiently prevents entry in the CNS of activated T cells, but also of B cells and myeloid cells (30). Moreover, CD8 T cell migration into the CNS has been shown to rely on the α4β1 integrin in murine models of CNS autoimmunity (13, 31). In our PCD mouse model, the α4 integrin is expressed on CD4 and CD8 T cells within the cerebellum; therefore, we considered treating with anti-α4 integrin antibody PS/2 at the onset of PCD. PS/2 administration did not provide any significant improvement in terms of clinical readouts and did not prevent T cell infiltration and killing of Purkinje cells. Different homing molecules may have a nonredundant role, depending on regional location of CNS lesions

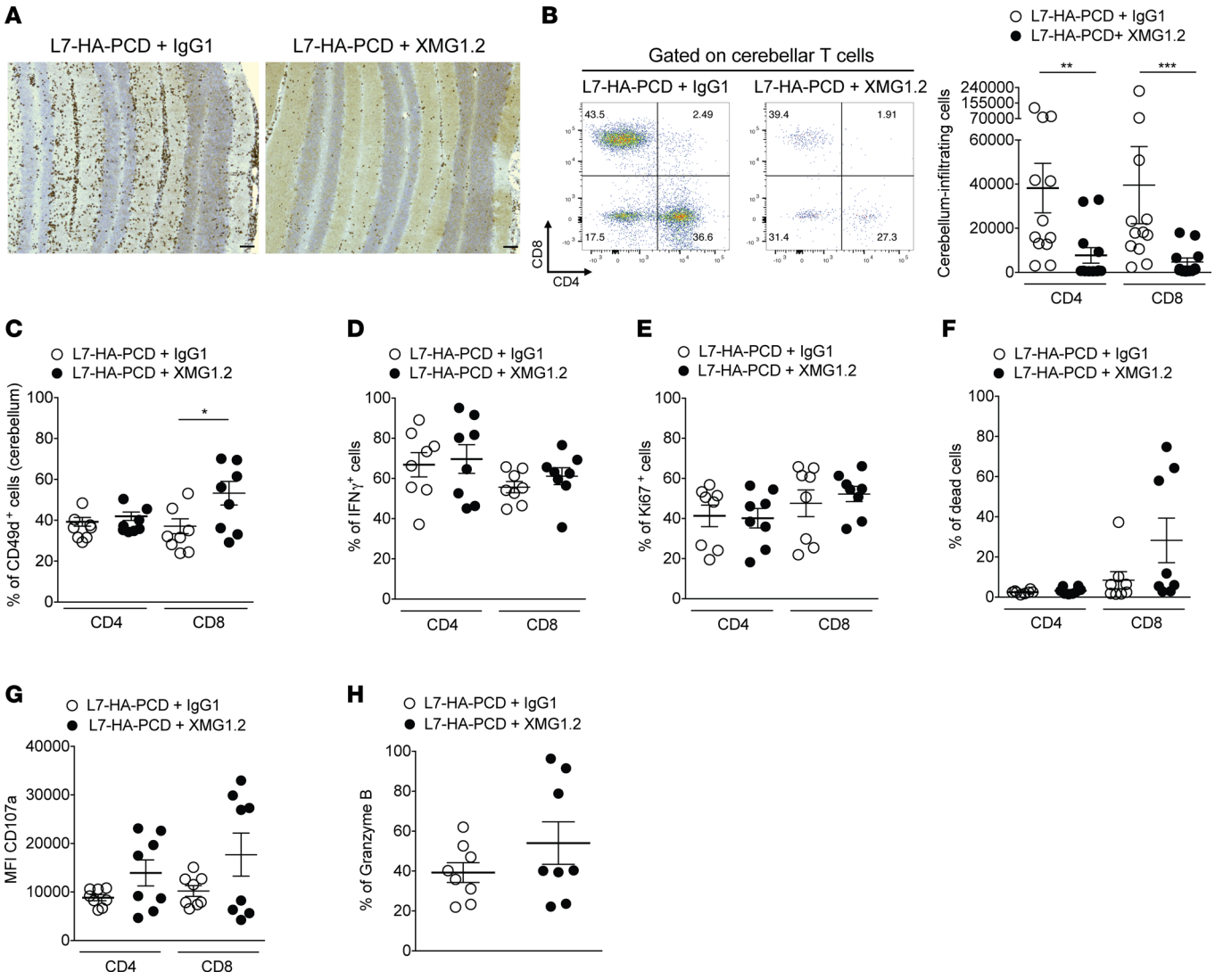

Figure 4. Cerebellar infiltration by T cells is reduced in PCD mice treated with anti–IFN-γ mAb. (**A**) Representative IHC for CD3⁺ cells (brown) with nuclear counterstaining with hematoxylin (blue) on cerebellar sections from L7-HA-PCD mice treated with XMG1.2 (neutralizing anti–IFN-γ mAb) or control IgG1. Scale bar: 100 μm. (**B**) Left: representative flow cytometry staining at day 16 for CD4 and CD8 gated on live cerebellum-infiltrating T cells (CD90.2⁺) from L7-HA-PCD mice treated with XMG1.2 or IgG1. Right: absolute numbers of CD4 and CD8 T cells infiltrating the cerebellum of L7-HA-PCD mice treated or not with XMG1.2 (n = 12 per group, 3 independent experiments; Mann-Whitney U test, $^{**}P < 0.01$; $^{***}P < 0.001$). (**C**) Expression of the α4 integrin (CD49d) on CD4 and CD8 T cells from the cerebellum of L7-HA-PCD mice treated with XMG1.2 or IgG1 (n = 8 per group, 2 independent experiments; Mann-Whitney U test, $^{*}P < 0.05$). Frequency of IFN-γ⁺ cells (**D**), proliferating (Ki67⁺) cells (**E**), and dead cells (**F**) among cerebellum-infiltrating CD4 and CD8 T cells of L7-HA-PCD mice treated with IgG1 or XMG1.2 (n = 8 per group, 2 independent experiments). Geomean of CD107a cells (**G**) and frequency of Granzyme B⁺CD8⁺ cells (**H**) among cerebellum-infiltrating T cells of L7-HA-PCD mice treated with IgG1 or XMG1.2 (n = 8 per group, 2 independent experiments).

and on the nature of immune cells responsible for tissue damage. Indeed, a different pattern of VCAM1 upregulation occurs in the spinal cord and cerebellum during EAE (32), which could relate to the lack of effect of anti–α4 integrin mAb in our model of cerebellar inflammation. Moreover, mouse Th17 cells can enter the CNS in an α4 integrin–independent mechanism, whereas Th1 cells strongly depend on α4 integrin for their entry (33, 34). We cannot, however, rule out a possible beneficial effect of anti–α4 integrin therapy in human PCD. Indeed, a patient with limbic encephalitis and anti-Hu antibodies, developing after anti-PD1 and anti–CTLA-4 therapy, responded well to natalizumab (35). Our data suggest that other molecules involved in T cell migration to the CNS could be involved. For example, a chemokine receptor, CCR5, has been suggested in CD8 T cell–driven neuroinflammation, as exemplified in viral encephalitis (14). We postulated that trafficking of T cells into the CNS could be hampered by use of a CCR5 antagonist 5P12-RANTES in the PCD model. However, the treatment with 5P12-RANTES did not ameliorate the disease. This could

be explained by the weak expression of CCR5 on T cells that infiltrated in the cerebellum of PCD mice and/or by the redundancy in molecules important for T cell trafficking to the CNS. For instance, the levels of CXCL10, an IFN-γ–induced chemokine, are elevated in the CSF of PCD patients; therefore, the CXCL10/CXCR3 axis may contribute to the trafficking of T cells into the cerebellum of PCD patients (36). Furthermore, cytotoxic T cells encountering their antigen and producing IFN-γ in the CNS may be responsible for the increased levels of CXCL10 in the CSF from patients with PCD (36).

In the PCD preclinical model, we observed a marked antigen-specific production of IFN-γ by cerebellum-infiltrating T cells, and the therapeutic data indicate that IFN-γ plays a key role in the disease process. Since IFN-γ deficiency in HA-specific CD8 T cells did not abrogate the disease (Figure 3E), IFN-γ production by antigen-specific CD4 T cells and/or host CD8 T cells is sufficient for PCD progression in the mouse model.

Treatments using corticosteroids, plasmapheresis, i.v. immunoglobulin, rituximab, and more aggressive immunosuppressive approaches, such as tacrolimus or cyclophosphamide, are often ineffective in patients with PCD because irreversible neuronal damage occurs rapidly and in the early phase of the disease (37–39). The present study establishes that blocking of IFN-γ is a promising approach against PCD and possibly other T cell–mediated paraneoplastic neurological diseases. IFN-γ neutralization in our mouse model led to complete protection of Purkinje cells from cytotoxic T cells. The PCD mice were treated from day 10 onward, a time point at which the tumor had already been rejected. This feature differs from the human disease in which the tumor, although frequently small or undetectable at the time of PCD onset, eventually manifests. Importantly, IFN-γ is an essential effector cytokine for tumor immune rejection, and loss of IFN-γ production by T cells allows tumor growth and persistence (40). Differing from the usual form of human PCD, CTLA-4 blockade was needed to elicit our mouse model. It is, however, striking that an increasing number of studies now report on the development of paraneoplastic neurological diseases upon administration of immune checkpoint blockade (7, 41, 42). Anti–CTLA-4 mAb administration, which in our mouse model was required to elicit full control of tumor growth and also development of PCD, is known to increase IFN-γ production by T cells (43, 44). However, when mice were treated with anti–IFN-γ mAb from the induction of disease (day 0), uncontrolled growth of tumor developed. Additionally, the mice did not develop PCD, since the occurrence of PCD is intimately linked to an effective antitumor immune response. Cancer in patients with PCD is often diagnosed because of the neurological signs and sometimes presents a long period of tumor invisibility, becoming detectable years after PCD onset (45).

Interestingly, even though the PCD was abrogated in mice treated with anti–IFN-γ antibody at onset of disease, some T cells were nevertheless present in the cerebellum. These T cells did not differ qualitatively in terms of proliferation and IFN-γ production when compared with those from untreated animals. Of note, CD8 T cells in this condition presented significantly higher expression of α4 integrin when compared with the CD8 T cells from cerebellum of the IgG-treated group. It has been shown that antigen-specific T cells from both IFN-$\gamma^{-/-}$ and IFNGR$^{-/-}$ mice express higher levels of α4 integrin in comparison with WT controls (46). The increased expression of α4 integrin is also reported in T cells from mice treated with the anti–IFN-γ neutralizing antibody XMG1.2 (47). This raises the possibility that this VCAM-1/α4β1 integrin pathway of T cells recruitment might be employed in the absence of IFN-γ, leading to T cell migration into the cerebellum. This could explain why anti–IFN-γ therapy resulted in incomplete inhibition of T cell trafficking into the antigen-expressing site.

This study establishes IFN-γ as an essential molecule that drives PCD pathology in a mouse model of PCD. Together with our proof-of-principle for antibody blockade in PCD mice, these findings delineate a reasonable route for clinical translation. A humanized IFN-γ blocking antibody previously demonstrated efficacy and safety in clinical trials for Crohn's disease (48). Likewise, anti–IFN-γ antibody has been tested for SLE, in which the IFN-γ blockade led to diminishing levels of CXCL10, a key chemokine associated with lupus disease activity (49). Therefore, a plausible disease-promoting cascade involves IFN-γ and CXCL10 production that may result in recruitment of additional T cells into tissue. IFN-γ can also promote immune cell recruitment into the CNS by enhancing VCAM1 expression on brain endothelial cells. Another feed-forward loop driven by IFN-γ is the increased expression of MHC class I molecules on neurons (27, 50), which become susceptible to cytolytic granule–mediated cytolysis. Targeting IFN-γ, therefore, could help break this loop, blocking further T cell homing to the CNS. Recently, the US Food and Drug Administration

(FDA) granted the Breakthrough Therapy Designation for Emapalumab, a fully human monoclonal anti–IFN-γ antibody, for the treatment of primary hemophagocytic lymphohistiocytosis, a syndrome of excessive immune activation and progressive immune-mediated organ damage due to genetic defects in cell-mediated cytotoxicity (51). This could facilitate the exploratory administration of anti–IFN-γ antibody for PCD patients.

Methods

Mice. L7-HA, 6.5-TCR, CL4-TCR, and CL4-TCR IFN-γ–KO mice have been described previously (52–55). All mice were on a BALB/c background. Mice were kept in specific pathogen-free conditions.

Adoptive T cell transfer and induction of PCD in the mouse model. Naive HA-specific $CD25^{-}CD62L^{+}CD4^{+}$ and $CD62L^{+}CD8^{+}$ T cells were purified as described (9). Briefly, spleen and cLN were isolated from 6.5-TCR and CL4-TCR transgenic mice. Single cell suspensions were generated, and CD4 or CD8 T cells were enriched using Dynabeads Untouched mouse CD4 or CD8 cells kit (Invitrogen). Tregs were depleted from the CD4 population by incubating with the anti-CD25 (clone PC61) mAb (in house) . Naive T cells were selected by using CD62L microbeads (Miltenyi Biotec).

$CD25^{-}CD62L^{+}CD4^{+}$ and $CD62L^{+}CD8^{+}$ T cells (1×10^7 each) were adoptively transferred into L7-HA mice or littermate controls. The same day, L7-HA or control mice were injected s.c. in the flank with 1×10^5 4T1 breast cancer cells that express HA of the PR8/34 influenza virus (4T1-HA cells) resuspended in 100 μl of PBS. To induce the PCD model, L7-HA mice implanted with the 4T1-HA tumor cells were injected i.p. with anti–CTLA-4 mAb (clone UC10-4F10-11; 100 μg/ injection) (in house) every other day starting from the day of T cell transfer and 4T1-HA implantation (day 0), as previously described (9).

Treatments. All treatments were administered i.p. from day 10 after induction of PCD in L7-HA mice onward. The anti–α4 integrin mAb (clone PS/2, BioXCell) was injected every 3 days (250 μg/injection). The anti–IFN-γ mAb (XMG1.2; 100 μg/injection) (gift from NovImmune) was given every other day. Where indicated, mice were treated with XMG1.2 from day 0. NovImmune provided the XMG1.2 and IgG control.

The CCR5 antagonist (5P12-RANTES, 10 μg/injection) was injected every other day.

Clinical assessment. Tumors were measured daily during 20 days with a Vernier caliper, and the tumor size (width × length) was expressed in mm^2. Mice were evaluated daily for weight loss and neurological signs. Motor coordination was assessed with Rotarod (Bioseb) with acceleration from 4–40 rpm over a 600-second period. For training, mice were tested on 7 consecutive days. During the investigation period (from days 0–20), the latency to fall was measured daily. The value at day 0 represents the 100% value for the latency to fall. The cumulative score was calculated by the sum of latency to fall (in seconds) from days 0–20.

Purification of cerebellum-infiltrating mononuclear cells and flow cytometry analyses. Sixteen days after PCD induction, mice were perfused with PBS, and their cerebellum and secondary lymphoid organs were dissected. Cerebellar homogenates were digested for 40 minutes at 37°C with digestion buffer (RPMI 1640, collagenase D 2 mg/ml, DNAse I 0.2 mg/ml, N-a-Tosyl-L-lysine chloromethyl ketone hydrochloride 0.02 mg/ml) (Sigma). Cells were then collected with a Percoll gradient separation. Spleen and cLN were dissociated, and RBCs were lysed with lysis buffer (0.15 M NH4 CL, 1 mM KHCO3, 0.1 mM Na2 EDTA, 0.5 M, pH 7.2) (all from Sigma). Mononuclear cells were collected and used for flow cytometry staining.

The following fluorescent dye–conjugated antibodies were used for flow cytometry staining: anti-Thy1.2 (53-2.1, BD Biosciences), anti-CD8α (53-6.7, BD Biosciences), anti-CD4 (RM4-5, BD Biosciences), anti–IFN-γ (XMG1.2, BD Biosciences), anti-CD49d (R1-2, BD Biosciences), anti-CCR5 (HM-CCR5, Thermo Fisher Scientific), anti-Ki67 (B56, BD Biosciences), anti-CD107a (1D4B, Thermo Fisher), and anti–granzyme B (NGZB, Thermo Fisher Scientific) antibodies. For IFN-γ, granzyme B and CD107a staining, mononuclear cells were stimulated with $HA_{512–520}$ or a control H-2-K^d–binding peptide ($Cw3_{170–179}$) for CD8 T cells, and $HA_{110–119}$ or a control H-2-IA^d–binding peptide ($OVA_{323–339}$) for CD4 T cells in presence of 5 μg/ml of APC anti-CD107a and Monensin for 16 hours, prior to staining with antibodies against surface proteins followed by fixation and permeabilization and staining. Data were recorded on BD Fortessa (BD Biosciences) and analyzed with the FlowJo software (Tree Star Inc.).

IHC. Staining of cerebellar sections were performed as described (56, 57) using anti–calbindin D28K (1:2000, catalog CD38, Swant), anti–calbindin D28K (1:1000, catalog C9848, Sigma), anti-CD3 (1:200, SP7, Zytomed), anti-CD8 (1:100, 4SM15, Thermo Fisher Scientific), and anti-pSTAT1 (1:75, catalog 9167, Cell Signaling Technology) as primary antibodies. Quantification of Purkinje neurons per mm of

Purkinje cell layer was determined from equally sized cerebellar cortex regions and normalized for the length of the Purkinje cell layer, as described previously (9).

Organotypic cerebellar slice culture. Organotypic cerebellar slice cultures were performed as described previously (58). Briefly, 300-μm thick cerebellar parasagittal slices were cut from L7-HA pups (P9–P10) and cultured in Millicell (MilliporeSigma) membranes. After 7 days, the slices were treated or without IFN-γ (100 U/ml) for 24 hours. The fluorescence stainings were performed using rabbit anti–calbindin D28K (1:2000, Swant) and mouse anti-H-2K^d (1:500, Thermo Fisher Scientific) as primary antibodies, followed by anti–rabbit Alexa Fluor 594 (1:1000) or anti–mouse Alexa Fluor 488 (1:1000; Invitrogen) secondary antibodies. Organotypic cerebellar slices were mounted in Mowiol (MilliporeSigma), and images were acquired with 2-photon LSM 7 MP microscope (Zeiss). The images were analyzed by Image J (Image J 1.48v, NIH).

Statistics. Statistical analyses were performed using the Student's *t* test (2-tailed) or with the Mann-Whitney *U* test, depending on whether data distribution was normal or not. For tumor size and weight loss, data were analyzed using the 2-way ANOVA (post-hoc Sidak's multiple comparison test). The analyses were performed on Prism 6 (GraphPad Software). Groups were considered statistically different at $P < 0.05$. The data are represented as mean ± SEM.

Study approval. All procedures involving animals were in accordance with the European Union guidelines and were validated by the Paris ministry–approved ethics committee (Ministere de l'Education Nationale, de l'Enseignement Superieur et de la Recherche) for animal welfare (APAFIS#4278-2016022510595289 v7).

Author contributions

LY designed the study; generated, analyzed and interpreted data; and wrote the manuscript. BP and EM helped with in vivo experiments. MP and MBW provided the anti–CTLA-4 antibody. OH provided the 5P12-RANTES. JB performed the IHC. RL originated and supervised the study, discussed the results, and critically revised the manuscript.

Acknowledgments

We would like to thank Nicolas Blanchard, Frederic Masson, Anne Dejean, Abdelhadi Saoudi, and Daniel Gonzalez-Dunia for their valuable inputs on the manuscript. The authors acknowledge the technical assistance provided by CPTP Cytometry and Imaging facility and the histology and animal facility staff of US006. This work was supported by the Inserm, CNRS, Toulouse University, and grants from the French MS society (ARSEP), The Foundation pour la Recherche Médicale (FRM), the French Research Agency (ANR T-cell Mig), ERA-NET NEURON (Meltra-BBB), and Bristol Myers-Squibb Foundation.

Address correspondence to: Roland Liblau, Centre de Physiopathologie de Toulouse-Purpan Hospital, Place du Docteur Baylac TSA 40031, 31059 Toulouse Cedex 9, France. Phone: 33562744571; Email: roland.liblau@inserm.fr.

1. Dalmau J, Rosenfeld MR. Paraneoplastic syndromes of the CNS. *Lancet Neurol*. 2008;7(4):327–340.
2. Furneaux HM, et al. Selective expression of Purkinje-cell antigens in tumor tissue from patients with paraneoplastic cerebellar degeneration. *N Engl J Med*. 1990;322(26):1844–1851.
3. Albert ML, Darnell JC, Bender A, Francisco LM, Bhardwaj N, Darnell RB. Tumor-specific killer cells in paraneoplastic cerebellar degeneration. *Nat Med*. 1998;4(11):1321–1324.
4. Darnell JC, Albert ML, Darnell RB. Cdr2, a target antigen of naturally occuring human tumor immunity, is widely expressed in gynecological tumors. *Cancer Res*. 2000;60(8):2136–2139.
5. Vedeler CA, et al. Management of paraneoplastic neurological syndromes: report of an EFNS Task Force. *Eur J Neurol*. 2006;13(7):682–690.
6. Small M, et al. Genetic alterations and tumor immune attack in Yo paraneoplastic cerebellar degeneration. *Acta Neuropathol*. 2018;135(4):569–579.
7. Yshii LM, Hohlfeld R, Liblau RS. Inflammatory CNS disease caused by immune checkpoint inhibitors: status and perspectives. *Nat Rev Neurol*. 2017;13(12):755–763.
8. Williams TJ, et al. Association of Autoimmune Encephalitis With Combined Immune Checkpoint Inhibitor Treatment for Metastatic Cancer. *JAMA Neurol*. 2016;73(8):928–933.
9. Yshii LM, et al. CTLA4 blockade elicits paraneoplastic neurological disease in a mouse model. *Brain*. 2016;139(11):2923–2934.
10. Miller DH, et al. A controlled trial of natalizumab for relapsing multiple sclerosis. *N Engl J Med*. 2003;348(1):15–23.
11. Kemp KC, Dey R, Verhagen J, Scolding NJ, Usowicz MM, Wilkins A. Aberrant cerebellar Purkinje cell function repaired in vivo by fusion with infiltrating bone marrow-derived cells. *Acta Neuropathol*. 2018;135(6):907–921.
12. Yamashita A, Makita K, Kuroiwa T, Tanaka K. Glutamate transporters GLAST and EAAT4 regulate postischemic Purkinje

cell death: an in vivo study using a cardiac arrest model in mice lacking GLAST or EAAT4. *Neurosci Res*. 2006;55(3):264–270.
13. Martin-Blondel G, et al. Migration of encephalitogenic CD8 T cells into the central nervous system is dependent on the α4β1-integrin. *Eur J Immunol*. 2015;45(12):3302–3312.
14. Martin-Blondel G, Brassat D, Bauer J, Lassmann H, Liblau RS. CCR5 blockade for neuroinflammatory diseases--beyond control of HIV. *Nat Rev Neurol*. 2016;12(2):95–105.
15. Xiao Z, Mescher MF, Jameson SC. Detuning CD8 T cells: down-regulation of CD8 expression, tetramer binding, and response during CTL activation. *J Exp Med*. 2007;204(11):2667–2677.
16. Kreutzfeldt M, et al. Neuroprotective intervention by interferon-γ blockade prevents CD8+ T cell-mediated dendrite and synapse loss. *J Exp Med*. 2013;210(10):2087–2103.
17. Peterson K, Rosenblum MK, Kotanides H, Posner JB. Paraneoplastic cerebellar degeneration. I. A clinical analysis of 55 anti-Yo antibody-positive patients. *Neurology*. 1992;42(10):1931–1937.
18. Giometto B, et al. Sub-acute cerebellar degeneration with anti-Yo autoantibodies: immunohistochemical analysis of the immune reaction in the central nervous system. *Neuropathol Appl Neurobiol*. 1997;23(6):468–474.
19. Albert ML, Austin LM, Darnell RB. Detection and treatment of activated T cells in the cerebrospinal fluid of patients with paraneoplastic cerebellar degeneration. *Ann Neurol*. 2000;47(1):9–17.
20. Santomasso BD, et al. A T-cell receptor associated with naturally occurring human tumor immunity. *Proc Natl Acad Sci USA*. 2007;104(48):19073–19078.
21. Scharton TM, Scott P. Natural killer cells are a source of interferon gamma that drives differentiation of CD4+ T cell subsets and induces early resistance to Leishmania major in mice. *J Exp Med*. 1993;178(2):567–577.
22. Szabo SJ, Sullivan BM, Stemmann C, Satoskar AR, Sleckman BP, Glimcher LH. Distinct effects of T-bet in TH1 lineage commitment and IFN-gamma production in CD4 and CD8 T cells. *Science*. 2002;295(5553):338–342.
23. Bien CG, et al. Destruction of neurons by cytotoxic T cells: a new pathogenic mechanism in Rasmussen's encephalitis. *Ann Neurol*. 2002;51(3):311–318.
24. Panitch HS, Hirsch RL, Haley AS, Johnson KP. Exacerbations of multiple sclerosis in patients treated with gamma interferon. *Lancet*. 1987;1(8538):893–895.
25. Harigai M, Kawamoto M, Hara M, Kubota T, Kamatani N, Miyasaka N. Excessive production of IFN-gamma in patients with systemic lupus erythematosus and its contribution to induction of B lymphocyte stimulator/B cell-activating factor/TNF ligand superfamily-13B. *J Immunol*. 2008;181(3):2211–2219.
26. Chevalier G, et al. Neurons are MHC class I-dependent targets for CD8 T cells upon neurotropic viral infection. *PLoS Pathog*. 2011;7(11):e1002393.
27. Di Liberto G, et al. Neurons under T Cell Attack Coordinate Phagocyte-Mediated Synaptic Stripping. *Cell*. 2018;175(2):458–471.e19.
28. Yednock TA, Cannon C, Fritz LC, Sanchez-Madrid F, Steinman L, Karin N. Prevention of experimental autoimmune encephalomyelitis by antibodies against alpha 4 beta 1 integrin. *Nature*. 1992;356(6364):63–66.
29. Engelhardt B, Laschinger M, Schulz M, Samulowitz U, Vestweber D, Hoch G. The development of experimental autoimmune encephalomyelitis in the mouse requires alpha4-integrin but not alpha4beta7-integrin. *J Clin Invest*. 1998;102(12):2096–2105.
30. Niino M, et al. Natalizumab effects on immune cell responses in multiple sclerosis. *Ann Neurol*. 2006;59(5):748–754.
31. Ifergan I, et al. Central nervous system recruitment of effector memory CD8+ T lymphocytes during neuroinflammation is dependent on α4 integrin. *Brain*. 2011;134(Pt 12):3560–3577.
32. Archambault AS, Sim J, McCandless EE, Klein RS, Russell JH. Region-specific regulation of inflammation and pathogenesis in experimental autoimmune encephalomyelitis. *J Neuroimmunol*. 2006;181(1-2):122–132.
33. Rothhammer V, et al. Th17 lymphocytes traffic to the central nervous system independently of α4 integrin expression during EAE. *J Exp Med*. 2011;208(12):2465–2476.
34. Rothhammer V, et al. α4-integrins control viral meningoencephalitis through differential recruitment of T helper cell subsets. *Acta Neuropathol Commun*. 2014;2:27.
35. Hottinger AF, de Micheli R, Guido V, Karampera A, Hagmann P, Du Pasquier R. Natalizumab may control immune checkpoint inhibitor-induced limbic encephalitis. *Neurol Neuroimmunol Neuroinflamm*. 2018;5(2):e439.
36. Roberts WK, Blachère NE, Frank MO, Dousmanis A, Ransohoff RM, Darnell RB. A destructive feedback loop mediated by CXCL10 in central nervous system inflammatory disease. *Ann Neurol*. 2015;78(4):619–629.
37. Keime-Guibert F, et al. Treatment of paraneoplastic neurological syndromes with antineuronal antibodies (Anti-Hu, anti-Yo) with a combination of immunoglobulins, cyclophosphamide, and methylprednisolone. *J Neurol Neurosurg Psychiatry*. 2000;68(4):479–482.
38. Vernino S, O'Neill BP, Marks RS, O'Fallon JR, Kimmel DW. Immunomodulatory treatment trial for paraneoplastic neurological disorders. *Neuro-oncology*. 2004;6(1):55–62.
39. Shams'ili S, et al. An uncontrolled trial of rituximab for antibody associated paraneoplastic neurological syndromes. *J Neurol*. 2006;253(1):16–20.
40. Dunn GP, Koebel CM, Schreiber RD. Interferons, immunity and cancer immunoediting. *Nat Rev Immunol*. 2006;6(11):836–848.
41. Matsuoka H, et al. Nivolumab-induced Limbic Encephalitis with Anti-Hu Antibody in a Patient With Advanced Pleomorphic Carcinoma of the Lung. *Clin Lung Cancer*. 2018;19(5):e597–e599.
42. Papadopoulos KP, Romero RS, Gonzalez G, Dix JE, Lowy I, Fury M. Anti-Hu-Associated Autoimmune Limbic Encephalitis in a Patient with PD-1 Inhibitor-Responsive Myxoid Chondrosarcoma. *Oncologist*. 2018;23(1):118–120.
43. Liakou CI, et al. CTLA-4 blockade increases IFNgamma-producing CD4+ICOShi cells to shift the ratio of effector to regulatory T cells in cancer patients. *Proc Natl Acad Sci USA*. 2008;105(39):14987–14992.
44. Fu T, He Q, Sharma P. The ICOS/ICOSL pathway is required for optimal antitumor responses mediated by anti-CTLA-4 therapy. *Cancer Res*. 2011;71(16):5445–5454.
45. Mathew RM, Cohen AB, Galetta SL, Alavi A, Dalmau J. Paraneoplastic cerebellar degeneration: Yo-expressing tumor

revealed after a 5-year follow-up with FDG-PET. *J Neurol Sci*. 2006;250(1-2):153–155.
46. Turner SJ, Olivas E, Gutierrez A, Diaz G, Doherty PC. Disregulated influenza A virus-specific CD8+ T cell homeostasis in the absence of IFN-gamma signaling. *J Immunol*. 2007;178(12):7616–7622.
47. Baumgarth N, Kelso A. In vivo blockade of gamma interferon affects the influenza virus-induced humoral and the local cellular immune response in lung tissue. *J Virol*. 1996;70(7):4411–4418.
48. Hommes DW, et al. Fontolizumab, a humanised anti-interferon gamma antibody, demonstrates safety and clinical activity in patients with moderate to severe Crohn's disease. *Gut*. 2006;55(8):1131–1137.
49. Welcher AA, et al. Blockade of interferon-gamma normalizes interferon-regulated gene expression and serum CXCL10 levels in patients with systemic lupus erythematosus. *Arthritis Rheumatol*. 2015;67(10):2713–2722.
50. Neumann H, Schmidt H, Cavalié A, Jenne D, Wekerle H. Major histocompatibility complex (MHC) class I gene expression in single neurons of the central nervous system: differential regulation by interferon (IFN)-gamma and tumor necrosis factor (TNF)-alpha. *J Exp Med*. 1997;185(2):305–316.
51. Al-Salama ZT. Emapalumab: First Global Approval. *Drugs*. 2019;79(1):99–103.
52. Kirberg J, Baron A, Jakob S, Rolink A, Karjalainen K, von Boehmer H. Thymic selection of CD8+ single positive cells with a class II major histocompatibility complex-restricted receptor. *J Exp Med*. 1994;180(1):25–34.
53. Morgan DJ, et al. CD8(+) T cell-mediated spontaneous diabetes in neonatal mice. *J Immunol*. 1996;157(3):978–983.
54. Saito H, Tsumura H, Otake S, Nishida A, Furukawa T, Suzuki N. L7/Pcp-2-specific expression of Cre recombinase using knock-in approach. *Biochem Biophys Res Commun*. 2005;331(4):1216–1221.
55. Saxena A, et al. Cutting edge: Multiple sclerosis-like lesions induced by effector CD8 T cells recognizing a sequestered antigen on oligodendrocytes. *J Immunol*. 2008;181(3):1617–1621.
56. Bien CG, et al. Immunopathology of autoantibody-associated encephalitides: clues for pathogenesis. *Brain*. 2012;135(Pt 5):1622–1638.
57. Bauer J, Lassmann H. Neuropathological Techniques to Investigate Central Nervous System Sections in Multiple Sclerosis. *Methods Mol Biol*. 2016;1304:211–229.
58. Ghoumari AM, Wehrlé R, De Zeeuw CI, Sotelo C, Dusart I. Inhibition of protein kinase C prevents Purkinje cell death but does not affect axonal regeneration. *J Neurosci*. 2002;22(9):3531–3542.